



Hippocampal rhythms affected by the GABA_AR β_3 subunit

H. Hentschke¹, M.I. Banks¹, M.G. Perkins¹, G.E. Homanics², R.A. Pearce¹

1. Department of Anesthesiology, University of Wisconsin, Madison WI 53706, USA

2. Department of Anesthesiology, University of Pittsburgh School of Medicine, Pittsburgh PA 15261, USA

Introduction

- The rodent hippocampus displays distinct field potential rhythms (θ , 4-12 Hz; γ , 30-80 Hz; ripples, ~200 Hz)
- θ oscillations in the CA1 subfield are presumably driven by two generators whose synaptic inputs produce spatially segregated pairs of current sinks and sources (in stratum pyramideale and stratum lacunosum-moleculare, respectively). Both generators are phase-shifted relative to each other, producing the gradual phase shift of θ across hippocampal layers

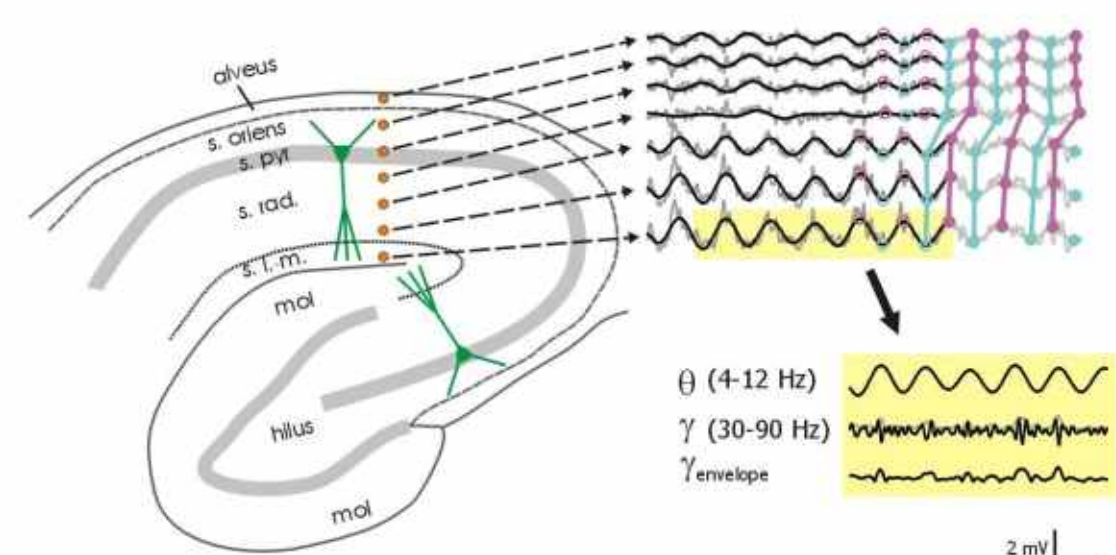
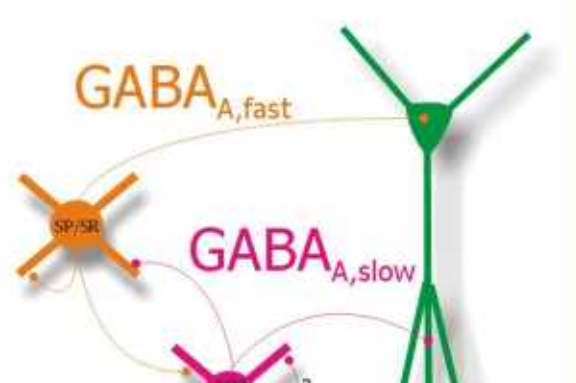
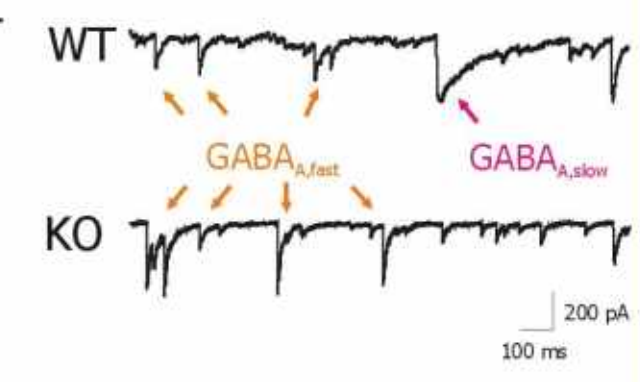


Figure 1 Prototypical local field potential activity recorded from mouse hippocampus. θ oscillations (4-12 Hz) and γ oscillations (30-90 Hz) are observed throughout the hippocampal layers; their amplitudes are highest at the fissure/stratum lacunosum-moleculare (SLM). θ oscillations show a gradual phase shift of slightly less than half a period from SLM to the alveus. γ oscillation magnitude is modulated by the θ rhythm

- GABA_A mediated currents are among the key players in shaping/generating both θ and γ rhythms
- There is evidence for two types of GABA_A receptor-mediated inhibitory currents which are spatially segregated and pharmacologically different and may subserve different functions (Pearce 1993, Banks et al 1998): GABA_{A, fast}, due to somatic inhibition, and GABA_{A, slow} located dendritically
- GABA_{A, slow} is largely reduced in β_3 knockouts (Banks et al 2001). Thus, it could be partially mediated by this subunit, which is abundant in dendritic layers of hippocampus (Sperk et al 1997)
- GABA_{A, slow} suppresses GABA_{A, fast} (Banks et al 2000), presumably contributing to both θ and nested θ/γ rhythms
- In β_3 knockouts recurrent inhibition in CA1 is reduced in a post-stimulus time window which is compatible with an absence of GABA_{A, slow} as the cause (Benkowitz et al, 2004)
- In the light of these results it is postulated that the absence of the β_3 subunit, possibly manifest in a strong reduction of GABA_{A, slow}, should affect θ oscillations and the nesting of γ with θ in the hippocampus vivo**



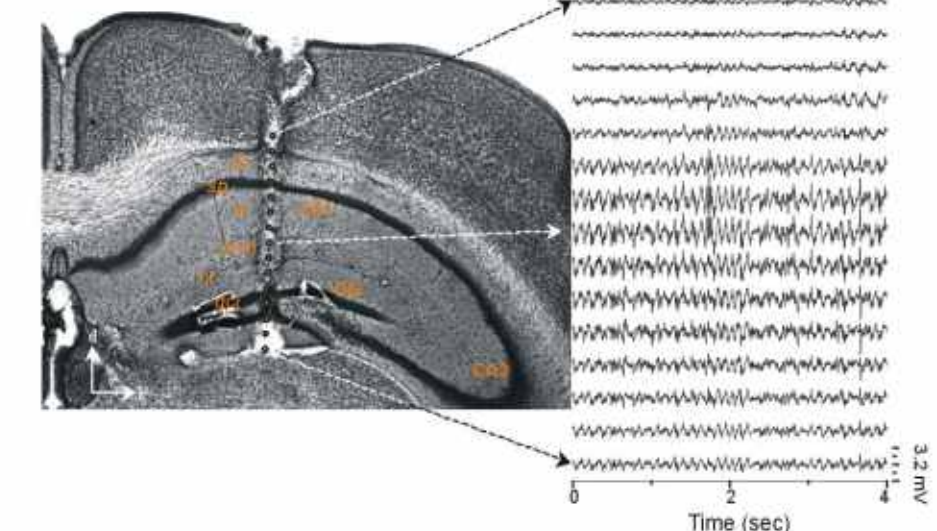
Methods

Electrode preparation and implantation

We used 15-channel linear NiChrome microwave arrays fabricated according to the technique of Jellema and Weijnen (1991). Wild types and β_3 knockouts (Homanics et al 1997) were chronically implanted with these electrodes under isoflurane anesthesia. The array was lowered into the left hippocampus (2.2 mm caudal to Bregma, 1.4 mm lateral to the midline) at a depth of 1.6 mm, such that the electrodes spanned hippocampus from the granule cell layer of the dentate gyrus to the alveus. The array was fixed on the head via three skull screws, one of which served as electrical ground, and dental acrylic. Animals were allowed to recover for one week before their first recording session. Electrode location was verified histologically.

Electrophysiology & behavioral scoring

For a recording session, a headstage was attached to the connector on the animal's head. The headstage was connected to amplifiers (Lynx-8, Neuralynx) via 30 gauge fine braided wire whose light weight and flexibility allowed the animals free range of movement. Local field potentials were recorded continuously from all active channels at a bandwidth of 1-300 Hz and sampled at 1 kHz using pClamp (Axon Instruments). The animals were allowed to move in an open plastic tray of 20 x 30 cm. They were videotaped and their behavior was scored offline or in parallel with the recording. Individual experimental sessions lasted ~30 min. An observer classified the animal's behavior as 'exploring' (locomotor activity), 'grooming' (including face- and paw-washing, eating and drinking) and 'immobile'. In practice, only 'immobile' and 'exploring' behaviors occurred with sufficient duration and frequency for data analysis.



Data analysis

Data analysis was performed with custom-written routines in Matlab. For each behavior, the corresponding field potential data were divided into segments of 4096 points, corresponding to ~4 s, overlapping by 4095/3 points. Data segments shorter than this duration (due to rapid switching of behavior) were discarded. Artifacts were detected by a simple threshold detector and excluded. Spectral and crosscorrelation parameters were computed from the 4096-point segments and averaged. Spectral analysis included determination of the coherence between channels (with SLM as reference) and power in distinct frequency bands (theta, 4-12 Hz; gamma, 30-90 Hz) and amplitude and frequency of theta peak. For crosscorrelation (CC) analyses the raw data were split up in theta and gamma streams via digital filtering (without phase shift), and CC were computed from these. Gamma envelope was calculated as the absolute of the Hilbert transform of the gamma stream. Two principal types of CC were computed: (i) intra-electrode CC (theta-gamma envelope) and (ii) between-electrodes CC (theta-theta, gamma-gamma, gamma envelope-gamma envelope). To test the significance of differences between wild types and knockouts we pursued a statistical approach usually used for the comparison of dose-response curves. We fitted functions (of e.g. sigmoidal shape in case of the theta and gamma lags) to the data and computed an F-value, from which a p-value could be derived (Motulsky & Christopoulos 2003). For all comparisons WT - KO only behaviorally matched segments of data were used.

γ in KO: dramatic reduction of amplitude

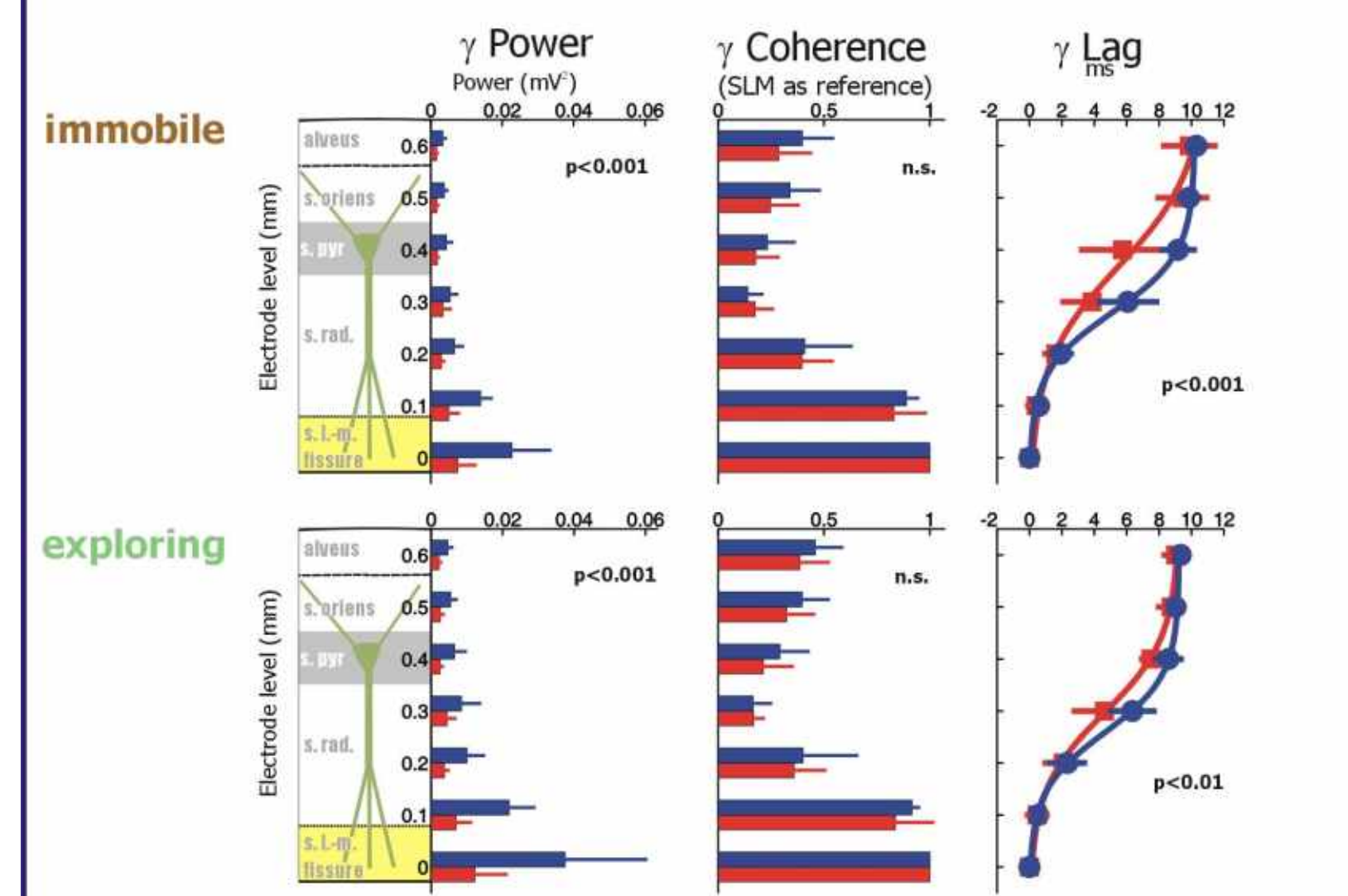


Figure 7 Comparison of γ oscillations in WT and KO. Although γ power is largely reduced in KO, particularly in SLM, coherence values between SLM and more dorsal sites are not significantly different in both genotypes. Note that the spatial profile of coherence values is qualitatively similar to that for θ . Line graphs (rightmost column) depict the phase shift of γ at each recording site relative to that at SLM. As θ , γ shows a gradual shift of phase from SLM to the alveus up to about half a period of the dominant frequency of the rhythm (10 ms, which would correspond to a frequency of ~50 Hz). In KO, slopes tended to be less steep than in WT, particularly during immobility.

γ envelope phase shifts peak in stratum radiatum and are larger in WT than in KO

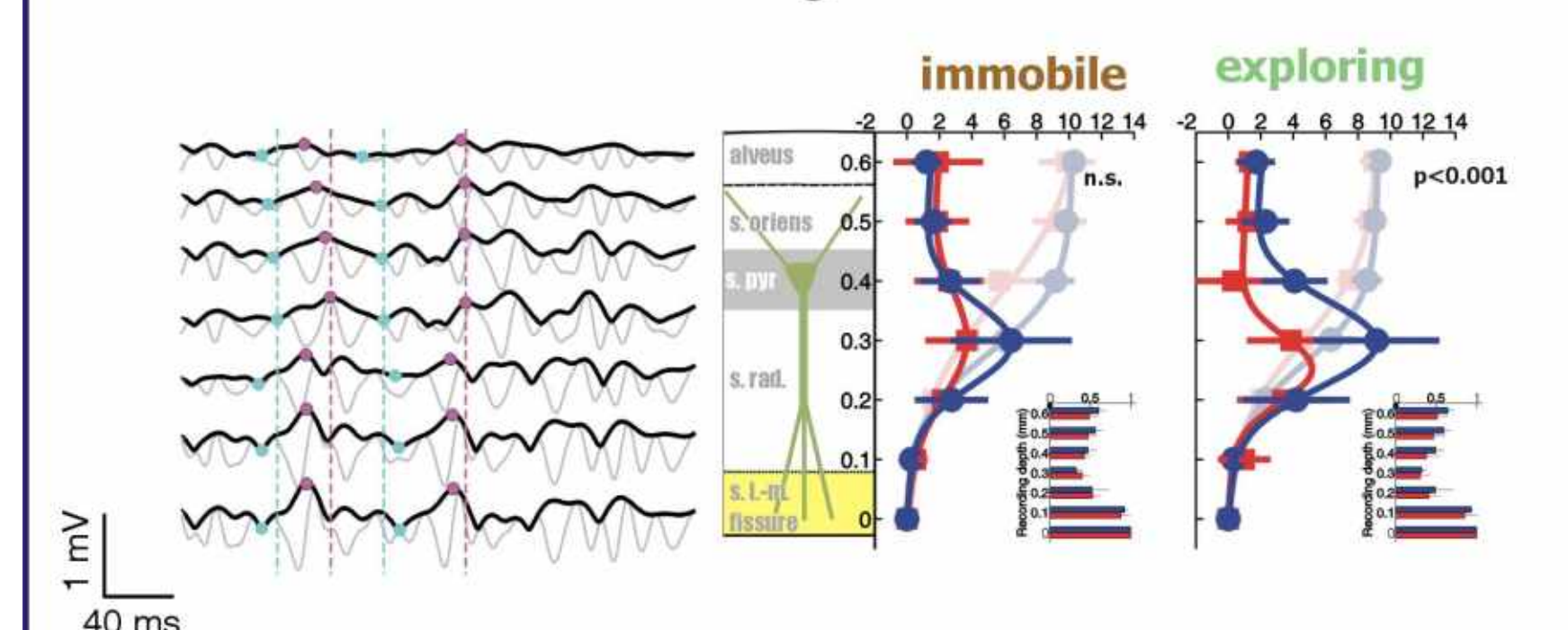


Figure 8 Left, γ and γ_{envelope} signals from a WT animal. Right, population data of phase shifts from all animals. Although γ showed a gradual, sigmoidal shift of phases (light traces in background) its magnitude followed a different pattern in both genotypes. In WT the lag at SR/SP was significantly larger than that of KO during exploration. Insets depict the strength of crosscorrelations.

θ and γ oscillations are more prominent during exploration than during immobility

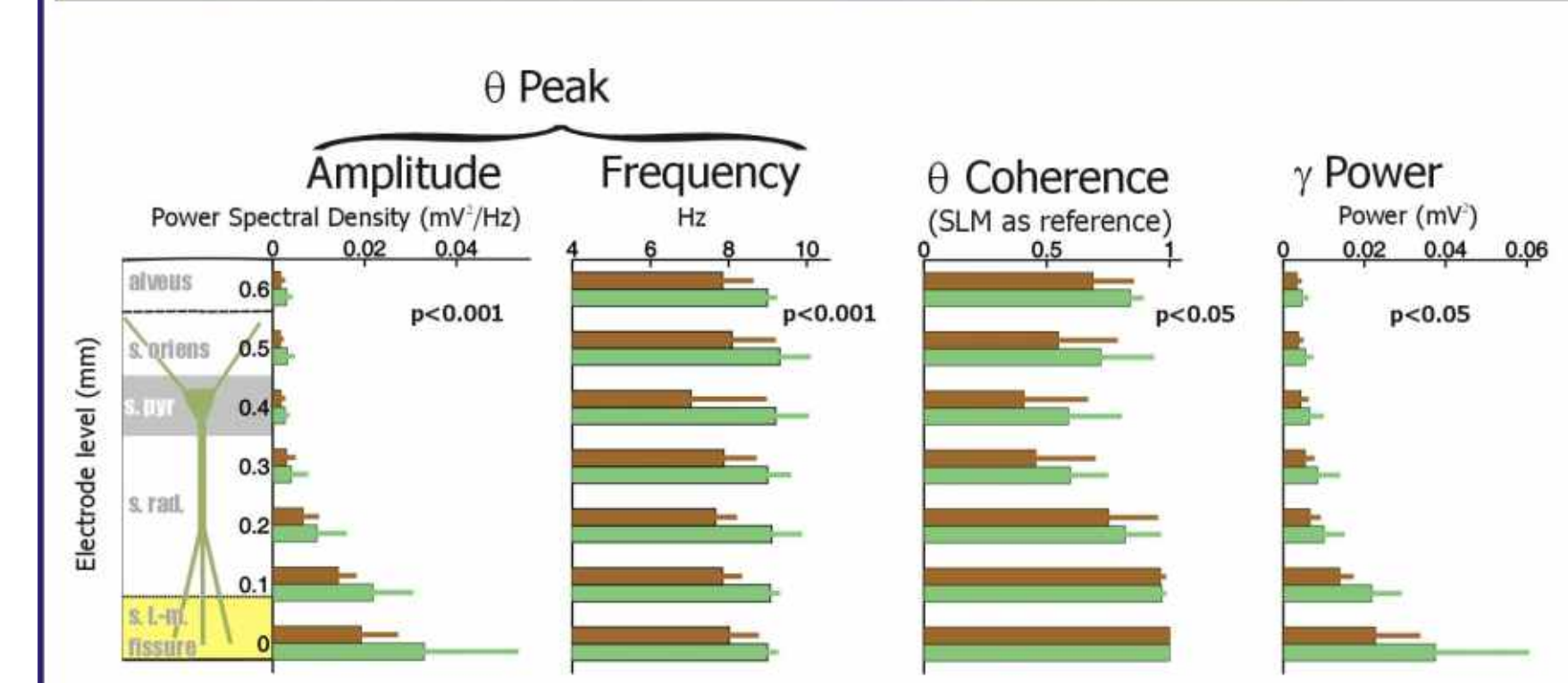
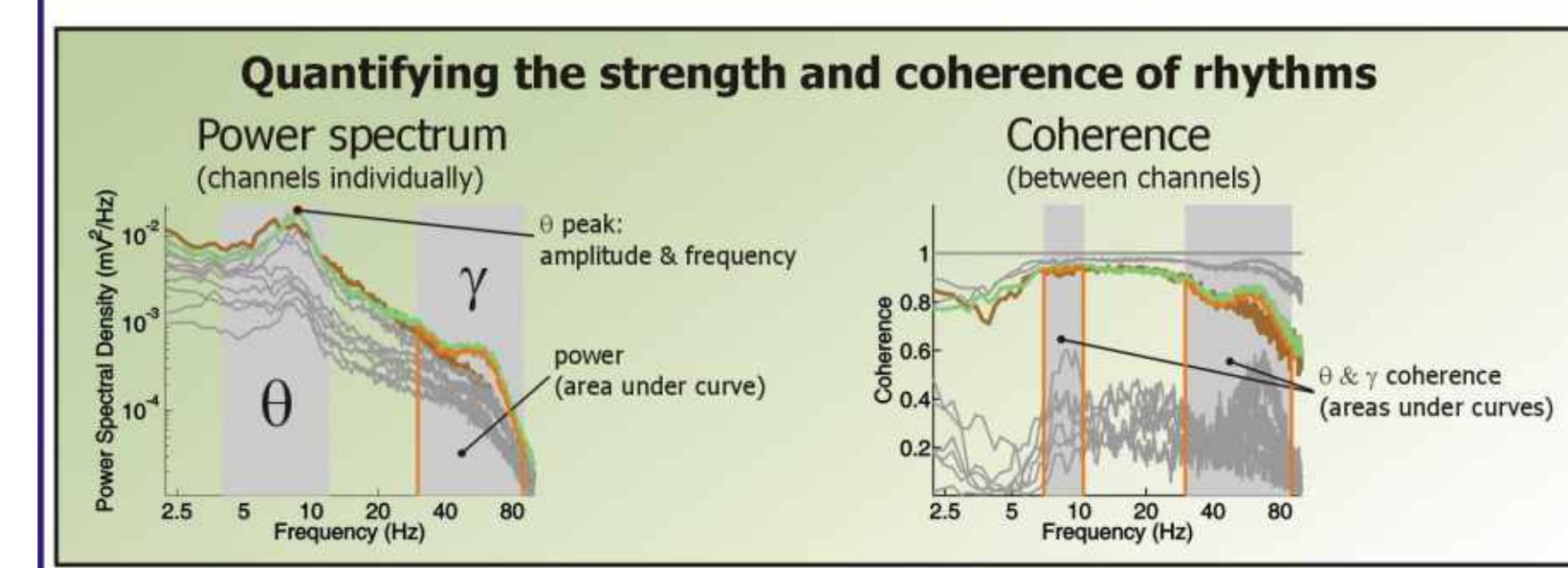
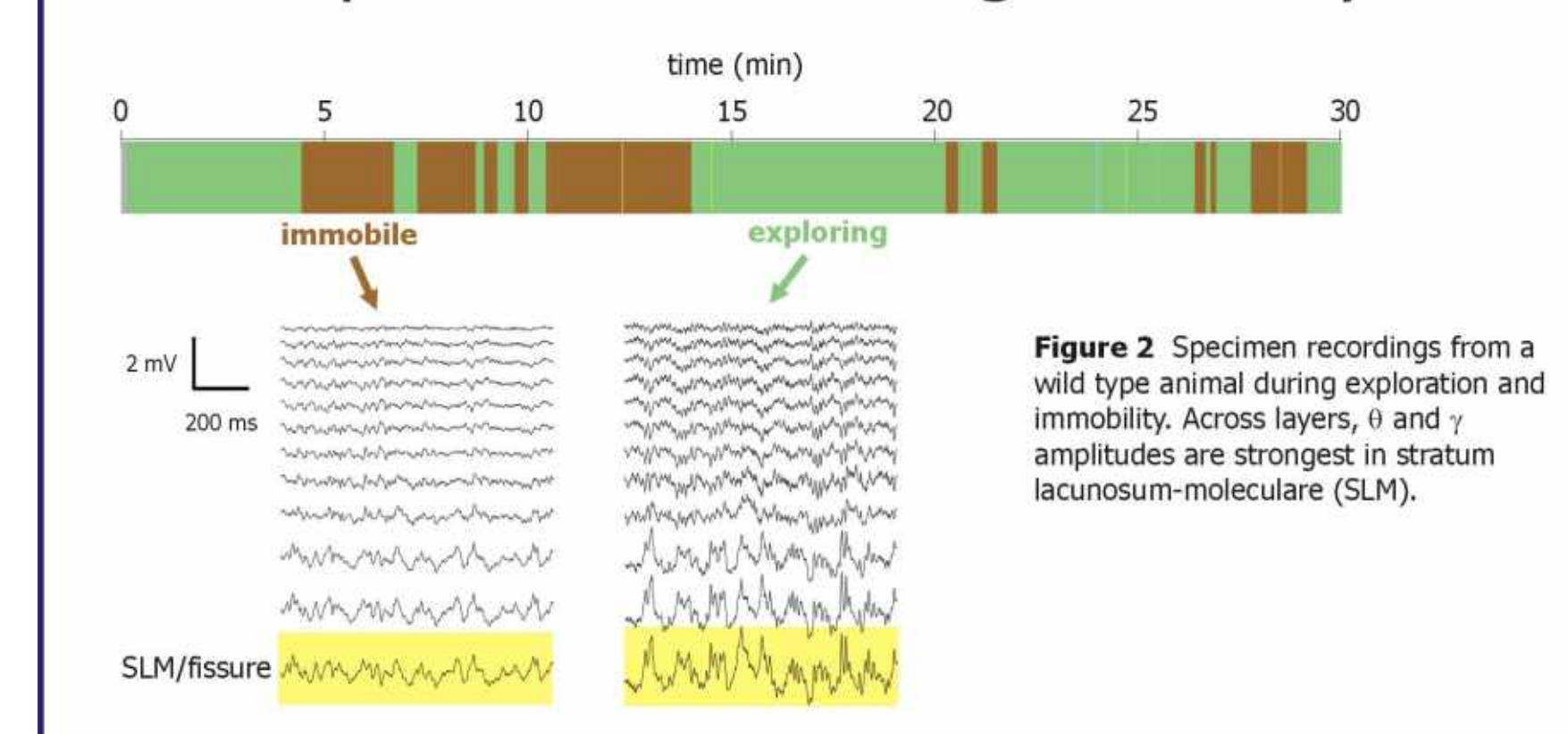


Figure 9 Specimen recordings from a wild type animal during exploration and immobility. The transition from this activity to theta oscillations was usually rapid. θ oscillations in KO were generally weaker, less similar among recording sites and on average less regular than in WT, but had a similar spatial amplitude profile (strongest amplitudes in SLM).

Figure 10 Averages of key parameters of θ and γ oscillations (n=7 WT). The differences between behaviors confirm findings in rats and make a comparison of behaviorally matched data segments between WT and KO mandatory

Interplay of the rhythms: less modulation of γ by θ in KO, but the temporal relation between the rhythms is the same

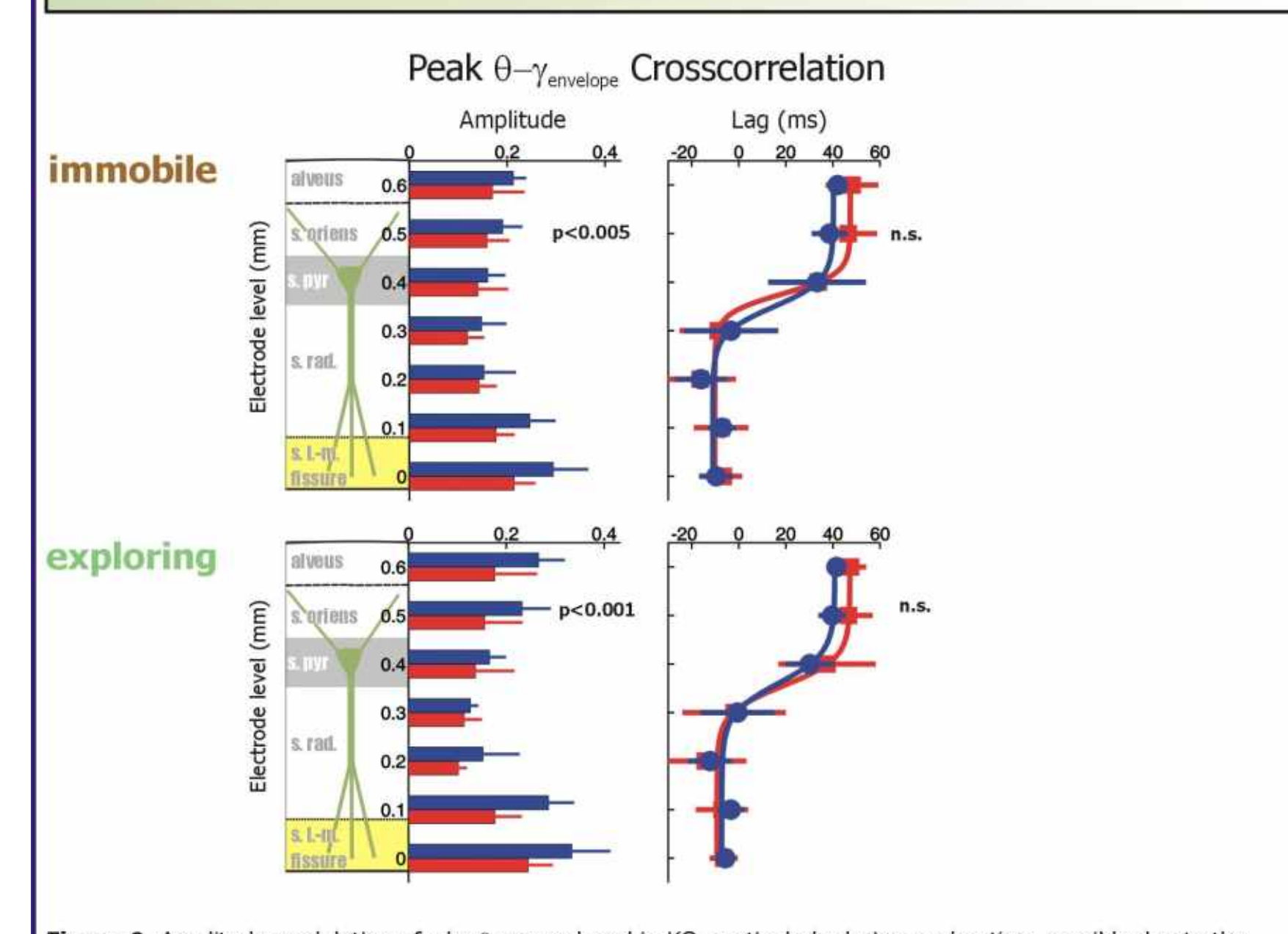
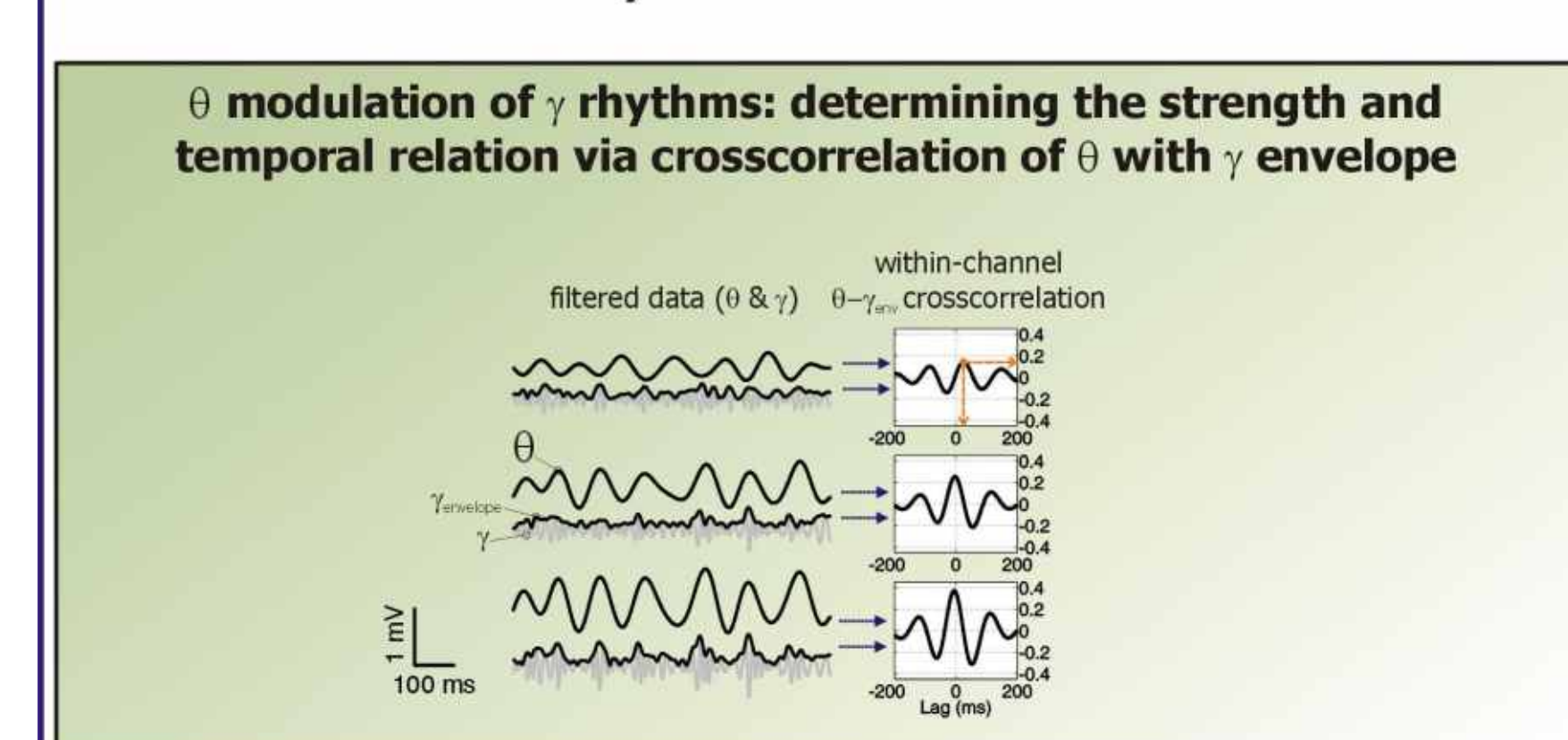


Figure 12 θ modulation of γ rhythms: determining the strength and temporal relation via crosscorrelation of θ with γ envelope

Figure 13 Amplitude modulation of γ by θ was reduced in KO, particularly during exploration, possibly due to the strong attenuation of θ and γ oscillations in these animals. However, the temporal relation of the rhythms (within each recording site) was virtually identical in both genotypes, largely reflecting the phase shift of θ across layers with respect to SLM: while in SLM γ preceded θ slightly, in SO/alveus it lagged by 40 ms.

θ oscillations are slower, weaker and less coherent across layers in knockouts

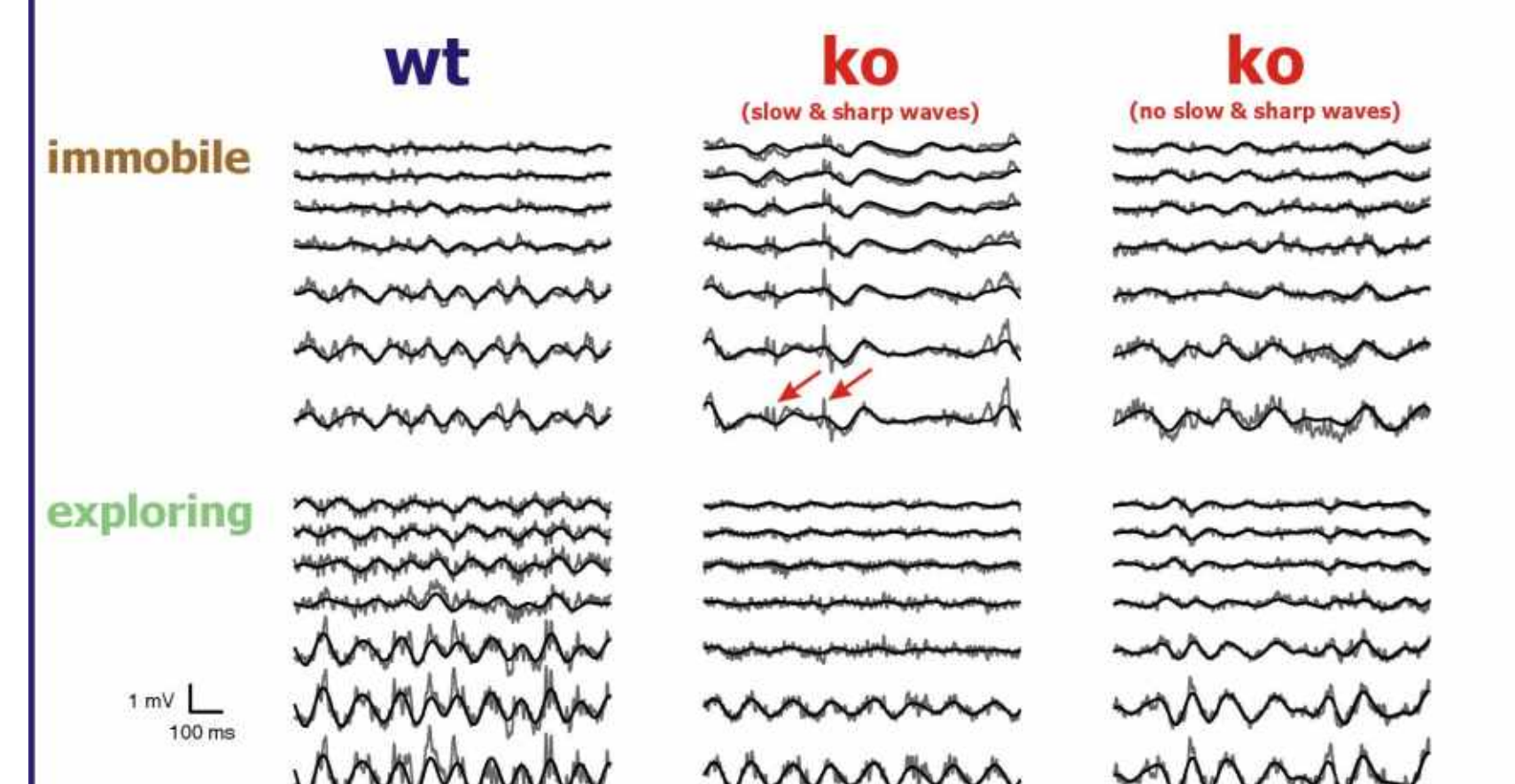


Figure 14 Specimen recordings from representative animals. 5 (of 8) KO showed occasional regular slow & sharp waves during immobility (see arrows in middle panel). The transition from this activity to theta oscillations was usually rapid. θ oscillations in KO were generally weaker, less similar among recording sites and on average less regular than in WT, but had a similar spatial amplitude profile (strongest amplitudes in SLM).

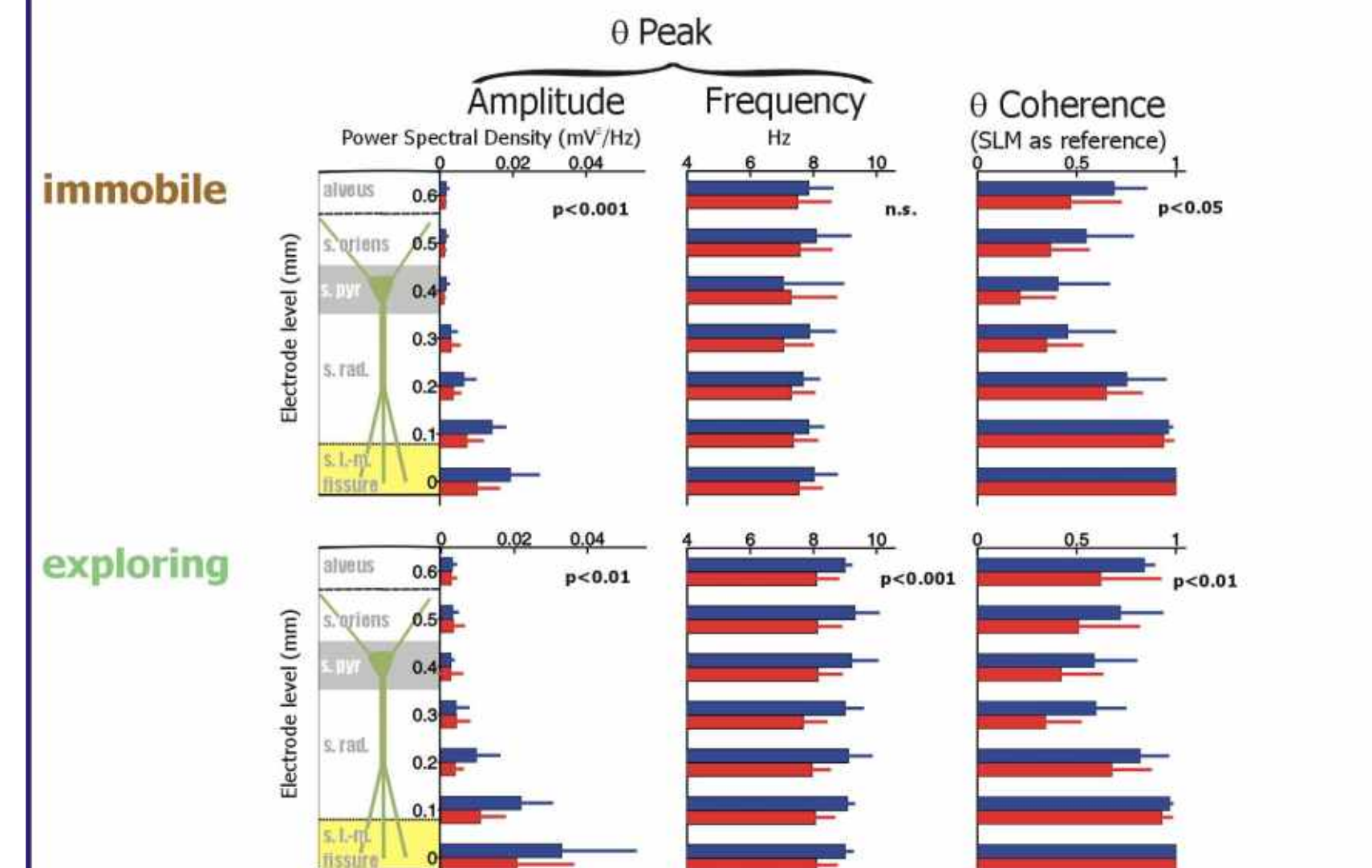
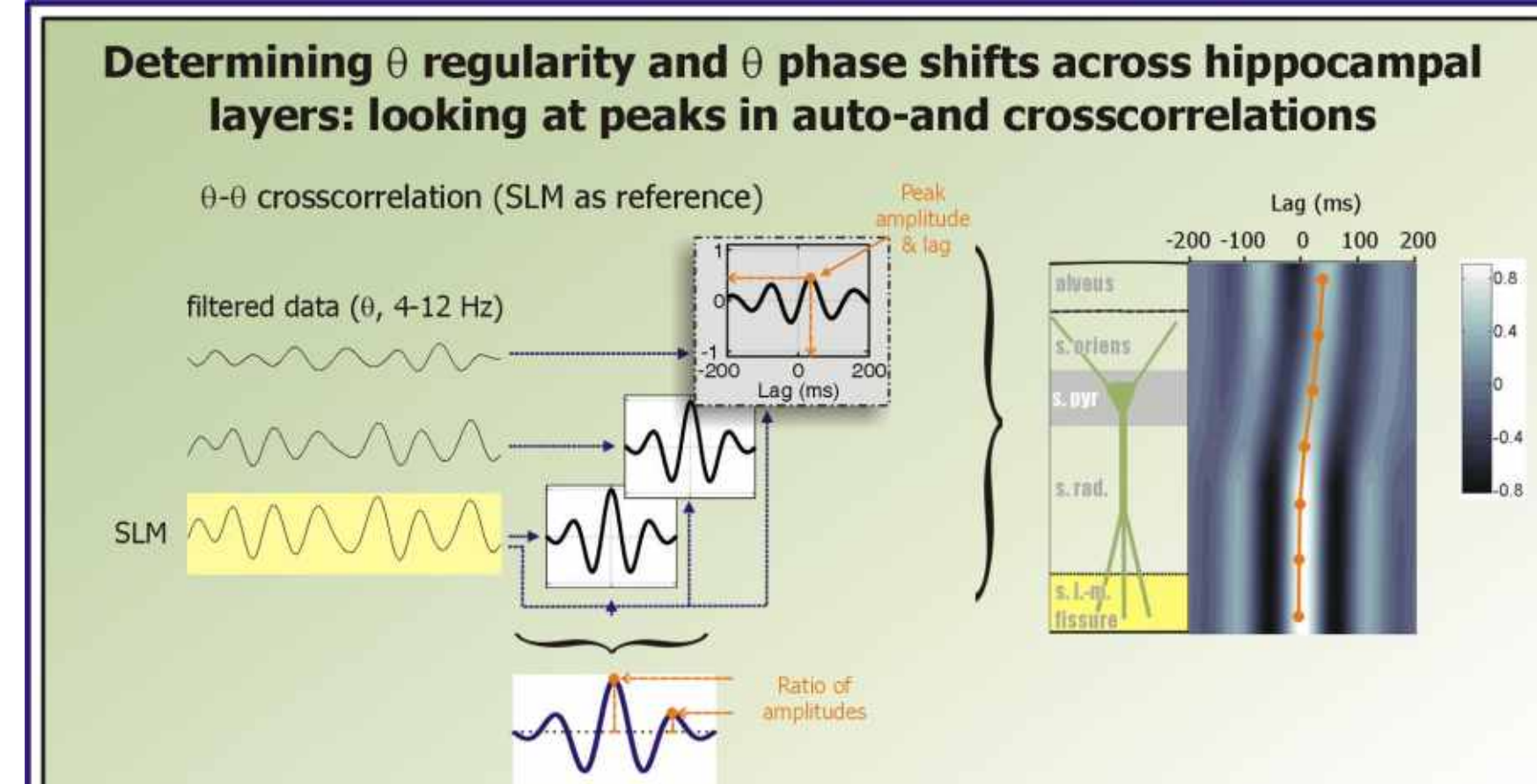


Figure 15 Comparison of key parameters of θ . The p-value applies to the null hypothesis of no differences between WT and KO derived from an F-test. See methods for details.



Determining θ regularity and θ phase shifts across hippocampal layers: looking at peaks in auto- and crosscorrelations

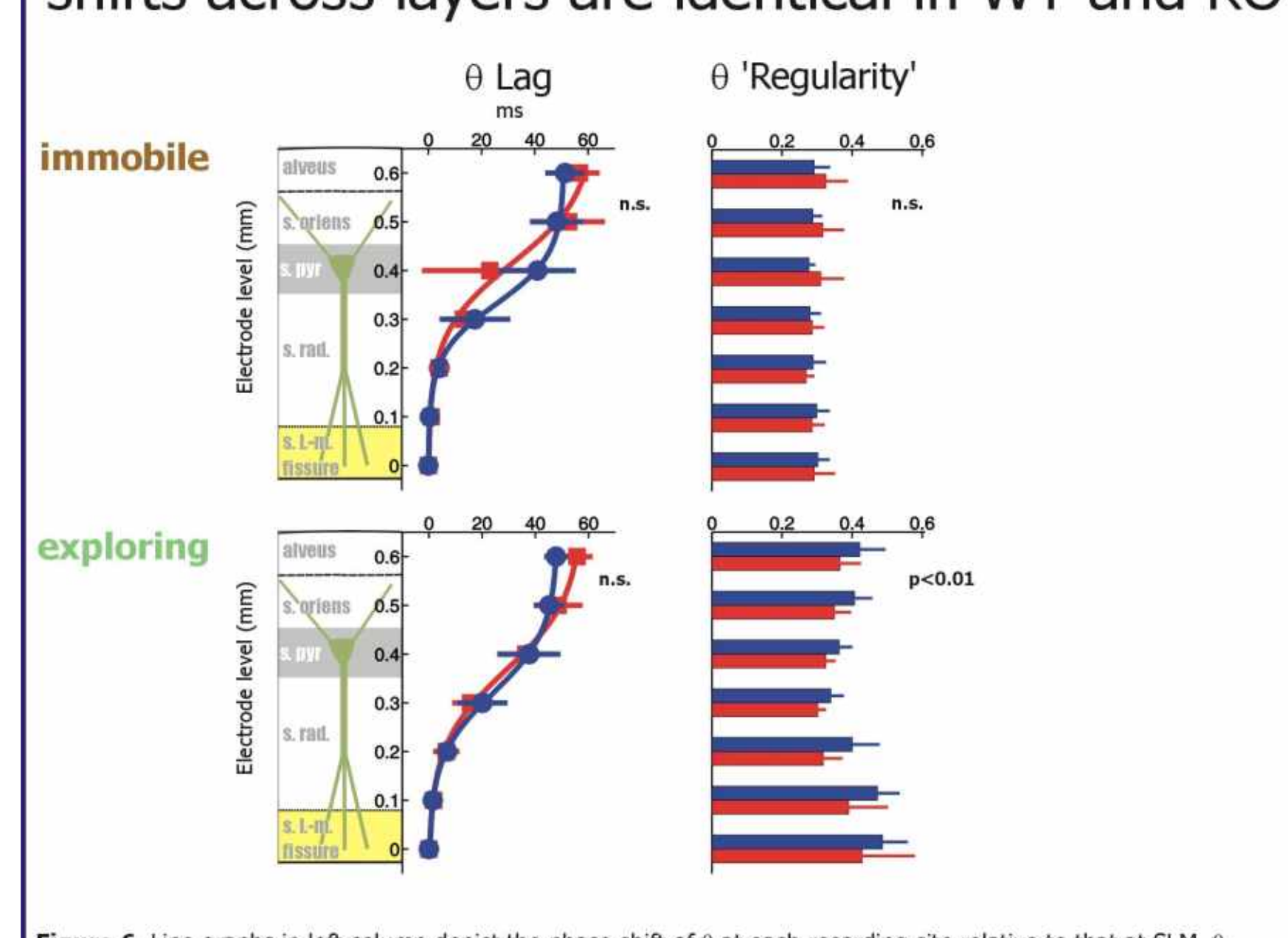


Figure 6 Line graphs in left column depict the phase shift of θ at each recording site relative to that at SLM. θ rhythms show a gradual shift of phase from SLM to the alveus of up to about half a period of the dominant frequency. Bar graphs in right column show the ratios of peak amplitudes in the autocorrelations of each site (largest sidepeak/central peak) as a crude measure of the regularity of θ .

Summary

- Two prominent hippocampal rhythms, θ and γ , are attenuated in β_3 knockouts, particularly in SLM
- in knockouts, θ rhythms are less well organized (less regular, less coherent among layers), but show a profile of laminar phase shifts undistinguishable from those in wildtypes
- modulation of γ by θ is less pronounced in KO, but the layer-specific temporal interplay between the rhythms is not affected
- most differences between genotypes tend to be more pronounced during exploratory behavior

- Taken together, our results are compatible with a role of slow inhibition in sculpting hippocampal θ rhythms and θ modulation of γ

References

- Banks MJ, Li T-B and Pearce RA. The synaptic basis of GABA_{A,slow}. J Neurosci 18: 1305-1327, 1998.
- Banks MJ, White JA and Pearce RA. Interactions between distinct GABA_A circuits in hippocampus. Neuron 25: 449-457, 2000.
- Banks MJ, Homanics GE, and Pearce RA. Reduced spontaneous and evoked GABA_{A,slow} IPSCs in mice lacking the β_3 subunit of the GABA_A receptor. Soc. Neuroscience Abstracts 2001.
- Benkowitz C, Homanics GE, and Pearce RA. Recurrent inhibition and its enhancement of etomidate differ in wild type versus GABA_A β_3 mice. Soc. Neuroscience Abstracts 2004.
- Homanics GE, Delorey TM, Firestone LL, Quinlan JJ, Handforth A, Harrison NL, Krasowski MD, Rick CE, Korpi ER, Makela R, Brilliant MH, Hagihara, Ferguson C, Snyder K and Olsen RW. Mice devoid of gamma-aminobutyrate type A receptor beta3 subunit have epilepsy, cleft palate, and hypersensitive behavior. Proceedings of the National Academy of Sciences of the United States of America 94: 4143-4148, 1997.
- Jellema T and Weijnen JA. A slim needle-shaped multiview microelectrode for intracerebral recording. J Neurosci Methods 40: 203-209, 1991.
- Motulsky HJ and Christopoulos A. Fitting models to biological data using linear and nonlinear regression. A practical guide to curve fitting. San Diego, CA: GraphPad Software Inc., 2003.
- Pearce RA. Physiological evidence for two distinct GABA responses in rat hippocampus. Neuron 10: 189-200, 1993.
- Sperk G, Schwarzer C, Tsunashima K, Fuchs K and Sieghart W. GABA(A) receptor subunits in the rat hippocampus I: immunocytochemical distribution of 13 subunits. Neuroscience 80: 987-1000, 1997.